IIETA International Information and Engineering Technology Association
Advancing the World of Information and Engineering

Revue des Composites et des Matériaux Avancés-Journal of Composite and Advanced Materials
Vol. 36, No. 1, February, 2026, pp. 13-26
Journal homepage: http://iieta.org/journals/rcma

Ballistic Impact Resistance of Hybrid Polymer Composites for Protective Shields: Experimental Evaluation Against 9 mm Projectiles

Rashid Faisal Mohammed*, Waleed Bdaiwi

Department of Physics, College of Education for Pure Science, University of Anbar, Ramadi 31001, Iraq

Corresponding Author Email: ras22u3008@uoanbar.edu.iq

https://doi.org/10.18280/rcma.360102

Received: 2 March 2025
Revised: 5 May 2025
Accepted: 15 February 2026
Available online: 28 February 2026

Keywords:
hybrid composites, ballistic impact, Kevlar reinforcement, energy absorption, personal armor, 9 mm projectile

ABSTRACT

The development of lightweight, high-performance armor remains a central challenge in personal protection engineering. This study experimentally evaluates hybrid polymer composites designed for protective shields against 9 mm full metal jacket (FMJ) projectiles in accordance with NIJ-0101.06 standards. Multi-layered composites incorporating Kevlar, carbon fibers, glass fibers, aluminum tread plates, and tanned cowhide leather were fabricated using a natural rubber-modified unsaturated polyester matrix. Mechanical properties were assessed through bending, compression, hardness, and Charpy impact testing, followed by field ballistic evaluation and X-ray imaging. Among five configurations, Sample 4 exhibited superior performance, achieving an impact strength of 23.5 kJ/m², bending strength of 115.67 MPa, and compressive strength of 117.9 MPa. Compared to the least-performing configuration, it demonstrated approximately 67% higher impact energy absorption and 75% improvement in flexural strength. X-ray analysis confirmed projectile entrapment without full penetration and revealed progressive delamination and fiber fracture as dominant energy-dissipation mechanisms. The synergistic interaction between high-toughness Kevlar layers, stiff carbon and glass fibers, elastomeric matrix modification, and a front aluminum plate enabled effective redistribution of kinetic energy. The proposed hybrid design offers a cost-effective and structurally efficient solution for handgun-threat protection applications.

1. INTRODUCTION

In the last decades, there has been intensive study on the development of advanced materials for protective applications, including in bullet-resistant shields [1-6]. One of the most difficult materials requirements is that these materials must possess a suite of mechanical properties such as high hardness, flexural strength, and compressive strength, as well as the ability to absorb and dissipate energy at the time of impact [7-11]. Materials available today with excellent ballistic resistance include metals and ceramics, but they tend to be heavy and rigid, unsuitable for applications with a need for mobility and ergonomic efficiency. This makes polymer-based composites an attractive alternative as they offer characteristics such as a lightweight nature, tunable mechanical properties, and adaptability in many configurations [12-14].

Unsaturated polyester resin (UPS) is widely used in polymeric systems for its easy processing, cost-effectiveness, and inherent mechanical strength [15]. Very often, UPS is modified with reinforcements and additives to meet demanding bullet-resistant application requirements. Natural rubber (NR) is an exceptionally rubbery and good energy absorbing material [16], whereas natural rubber (NR) offers excellent impact resistance and good energy absorbing functionality; Polymethyl methacrylate (PMMA) acts as a very hard and very stiff material and therefore performs the role of stiffener [17]. The combination of these components in an optimized ratio forms a hybrid matrix with increased mechanical performance for ballistic applications [18, 19].

High-strength-to-weight-ratio reinforcements, such as Kevlar fibers (KF), carbon fibers (CF) and glass fibers (GF), are widely purported for their exceptional strength-to-weight ratios and have found extensive usage of in composite systems for ballistic protection [20]. Moreover, the material can be stacked with additional layers such as natural cowhide leather (CL) and aluminum checker plates (AP), to achieve multi-layered penetration and deformation resistance [21, 22]. The strategic arrangement of these reinforcements in polymeric matrices can result in high-performance lightweight composites for protective applications [21].

Hybrid composites with natural and synthetic fibers for ballistic protection have undergone substantial progress in terms of the composite. For example, natural fiber composites provide obvious ecological and economic benefits and have already proven viable alternatives to fully synthetic systems in ballistic applications [23]. Natural fiber composites like pineapple leaf fiber (PALF) with synthetic reinforcement

could meet the Level III ballistic standard at lower costs [11]. Haro et al. [21] discovered that hybrid combinations of Kevlar and aluminum alloy, augmented with shear-thickening fluids (STFs), could absorb more energy in ballistic impacts.

Graphene oxide coatings also offer a unique way to enhance the interfacial adhesion and durability in natural fiber composites [18], and it is possible to embed mallow and jute fibers in epoxy matrices to provide low-cost alternatives for multilayered armour systems [24]. Furthermore, Naveen et al. [25] provided a mini review of the opportunity to use eco-friendly natural fibers such as curaua, jute, and sisal for the replacement of synthetic fibers within ballistic structures.

Despite these advancements, however, a gap exists in the exploration of composites combining several reinforcement layers, like Kevlar, carbon, and glass fibers, along with unconventional reinforcement materials such as cowhide leather and aluminum checker plate. Bichang'a et al. [26] review the influence of stacking sequences and nanofillers on hybrid composite performance, and yet the influence of delamination and layering configurations with real-world ballistic impacts remains unclear. Although Fonseca et al. [20] emphasized the role of reinforcement optimization for Kevlar-based composites in ballistic applications, their work did not consider unconventional reinforcements such as leather.

Despite advances in polymer and fiber-reinforced composites for ballistic applications, challenges remain in balancing structural rigidity, flexibility, and energy absorption. Conventional systems often rely solely on synthetic adhesives and single-fiber reinforcements, which may suffer from inadequate ductility, poor impact damping, or high production costs. This study introduces a novel approach by integrating a hybrid adhesive composed of UPS, NR, and CS with multi-layered fibers, including Kevlar, carbon, glass, and stainless-steel mesh. This combination offers a sustainable and tunable strategy to improve mechanical performance and ballistic resistance. The novelty lies in the strategic tailoring of adhesive properties and fiber architectures to achieve both flexibility and high impact resistance-essential attributes for next-generation lightweight armor systems.

Bending, compression, impact, and hardness measurements of the composites were performed to assess their mechanical properties, and X-ray images of the depth of penetration and evaluation of structural integrity after ballistic impacts were obtained. Their ballistic performance was comprehensively tested under field shooting trials at various distances to simulate practical conditions in the real world. This study integrates diverse reinforcements and evaluates their performance under controlled conditions to contribute to the development of lightweight, cost-effective materials for military, law enforcement, and civilian applications. Additionally, it serves as a basis for hybrid composite research in protective materials.

2. MATERIALS AND METHODS

2.1 Adhesive compound

The adhesive formulation used in this study was a formulation based on UPS from Industrial Chemicals & Resins Co. Ltd (ICR) in Saudi Arabia. UPS is a clear viscous liquid of approximate density 1.2 g cm−3 at room temperature. In order to accelerate the curing, industrial methyl ethyl ketone peroxide (PMEK), also manufactured by ICR, was added at a ratio of 2 g per 100 g of UPS resin.

Furthermore, thermosetting resin from Shiva Dental Products (MAARC), India, namely, PMMA was added at 1% by weight. PMMA exists as a white powder with a density of 1.2 g/cm³ and is activated with a hardener in a 1:2 ratio, transitioning from solid to liquid for improved adhesion.

Natural rubber (NR) was included at 20%, sourced from Diwaniya Rubber Products Company (MSR 10). NR was dissolved into a viscous liquid using toluene (C_7H_8), supplied by Alpha Kimica, India. The elastomeric properties of NR allow it to absorb and dissipate energy effectively under impact. At 20% volume fraction, NR contributes optimal flexibility and toughness to the adhesive matrix, enhancing impact resistance without significantly reducing stiffness. However, higher NR loadings compromise the matrix's uniformity, weakening interfacial bonding and diminishing load transfer efficiency.

2.2 Reinforcement materials

The reinforcement materials included [27]:

- Kevlar fabric (KF): From Songhan Plastic Technology Co., Ltd., Japan.
- Carbon fibers (CF): From Fiber Glast Developments Corp., USA.
- Glass fibers (GF): From Sichuan Weibo New Material Group Co., Ltd., China.
- Aluminum tread plate (AP): From Jinan Zhangyang Aluminum Co., Ltd., China.
- Tanned cowhide leather: Sourced from local markets.

The specifications of these materials are provided in Table 1, while Figures 1 (a-c) show the natural rubber (NR), cowhide leather (CL), and aluminum tread plate (AP), respectively.

(a) Natural rubber (NR)

(b) Aluminum tread plate (AP)

(c) Tanned cowhide leather (CL)

Figure 1. Images showing the materials used in the study

Table 1. Specifications of reinforcement materials [27]

Material	Property	Value
Aramid Kevlar® 49	Density (g/cm³)	1.44
	Tensile Strength (MPa)	3000
	Tensile Modulus (GPa)	112
	Elongation at Break (%)	2.4
	Temperature Resistance (°C)	25.0
	Moisture Absorption (%)	3.5
	Water Absorption (%)	3.5
	Tenacity (N/tex)	2.08
	Poisson's Ratio	0.36
Carbon Fibers	Tensile Modulus (dry)	33.0–41.5 MSI
	Tensile Strength (dry)	700–850 KSI
Glass Fibers	Roll Length	100 yards
	Color	Black
	Product Code	EWR4000-1000
	Unit Weight (g/m²)	400 ± 32
	Width (mm)	1000 ± 10
	Length (m)	100 ± 4
Aluminum Tread Plate	Product	Aluminum Tread Plate
	Alloy and Temper	1050H14
	Lot No	B01071623
	Specification	4 mm × 1200 mm × 2440 mm

2.3 Development of body armor systems

The body armor samples were fabricated using a precise manual casting and compression process to ensure uniformity, eliminate defects, and optimize bonding. The procedure is outlined as follows:

(1) Preparation of the Adhesive Base Material

- Mixing: A mixture of 79% UPS, 1% PMMA, and 20% natural rubber (NR) was prepared. The components were mechanically stirred at 1000 rpm for 10 minutes to achieve a homogeneous adhesive mixture.
- Addition of Catalyst: PMEK was added to the mixture at a concentration of 2 g per 100 g of adhesive to initiate the curing process.

(2) Layer Impregnation

Layer-by-Layer Application: Each layer of the supporting materials-Kevlar fibers (KF), carbon fibers (CF), glass fibers (GF), and tanned cowhide leather (CL)-was individually impregnated with the adhesive mixture. The adhesive was applied uniformly across the surface of each layer using a brush to ensure complete saturation.

(3) Layer Assembly

Sequential Stacking: The impregnated layers were sequentially stacked in a predefined order (as detailed in the sample configurations) within a mold measuring 21 × 21 cm². A front aluminum tread plate (AP) was positioned as the first layer to serve as the primary impact surface.

(4) Compression

Mechanical Pressing: The stacked layers were compressed using a mechanical press at a pressure of 2 MPa to ensure uniform bonding and eliminate air bubbles. Compression was maintained for 28 hours at room temperature (25 ± 2°C) to facilitate polymerization and proper layer integration.

(5) Curing

- Demolding: After compression, the samples were carefully removed from the mold to avoid damage.
- Post-Curing: The samples were cured at room temperature for an additional 72 hours to ensure complete polymerization of the adhesive and stabilization of the composite structure.

(6) Additional Quality Assurance Steps

- Excess Adhesive Removal: The edges of the layers were compressed to enable excess adhesive to be removed manually to ensure uniform layer thickness
- Void Detection: Post-compression, we visually inspected and corrected any resulting voids or surface irregularities.
- Weight and Thickness Measurements: After curing, each sample was weighed and its thickness measured to verify uniformity of the samples.

2.4 Sample configurations

Five samples were prepared with a base material composed of a mixture of 79% UPS, 1% PMMA, and 20% NR, which has been used as the adhesive to bond to the supporting layers. The samples have the following configurations [28]:

(1) Sample 1:

- A front layer of aluminum tread plate (AP), followed by four layers each of Kevlar fibers (KF), tanned cowhide leather (CL), carbon fibers (CF), and glass fibers (GF).
- Adhesive: The base material described earlier.

(2) Sample 2:

- Four layers each of glass fibers (GF), carbon fibers (CF), tanned cowhide leather (CL), and Kevlar fibers (KF), with a front aluminum tread plate (AP).
- Adhesive: The base material described earlier.

(3) Sample 3:

- Five layers each of Kevlar fibers (KF), tanned cowhide leather (CL), carbon fibers (CF), and glass fibers (GF), with a front aluminum tread plate (AP).
- Adhesive: The base material described earlier.

(4) Sample 4:

- Six layers each of Kevlar fibers (KF), tanned cowhide leather (CL), carbon fibers (CF), and glass fibers (GF), with a front aluminum tread plate (AP).
- Adhesive: The base material described earlier.

(5) Sample 5:

- Six layers each of Kevlar fibers (KF), glass fibers (GF), carbon fibers (CF), and tanned cowhide leather (CL), with a front aluminum tread plate (AP).
- Adhesive: The base material described earlier.

The hybrid configuration of Kevlar fibers, carbon fibers, and aluminum plates ensures effective redistribution of kinetic energy and prevents localized stress concentrations. Kevlar provides high energy absorption, carbon fibers contribute rigidity and structural integrity, and aluminum plates enhance surface resistance against projectile penetration.

The rationale for selecting specific layer configurations in Sample 4, as an example, was intentionally selected based on theoretical principles, supporting literature, and pilot testing. Research has established that alternating soft Kevlar or carbon fiber with hard glass fiber reinforcement layers enhances delamination and interfacial friction for energy dissipation [28]. Previous investigations have shown that hybrid composites featuring these designs provide superior ballistic protection while minimizing system weight [29].

Table 2 provides the specifications of the samples, given their layer thickness, total thickness, and total weight.

Table 2. Specifications of prepared body armor samples [27]

Sample	Materials Used	Number of Layers (KF, CL, CF, GF, AP)	Layer Thickness (cm)	Total Thickness (cm)	Total Weight (g)
Sample 1	KF, CL, CF, GF, AP	4, 4, 4, 4,1	0.052, 0.18, 0.05, 0.056, 0.4	2.0	983
Sample 2	GF, CF, CL, KF, AP	4, 4, 4, 4,1	0.056, 0.05, 0.18, 0.052, 0.4	2.0	983
Sample 3	KF, CL, CF, GF, AP	5, 5, 5, 5,1	0.052, 0.18, 0.05, 0.056, 0.4	2.1	994
Sample 4	KF, CL, CF, GF, AP	6, 6, 6, 6,1	0.052, 0.18, 0.05, 0.056, 0.4	2.4	1163
Sample 5	KF, GF, CF, CL, AP	6, 6, 6, 6,1	0.052, 0.056, 0.05, 0.18, 0.4	2.4	1165

Note: Kevlar fibers (KF), Cowhide Leather (CL), Carbon Fibers (CF), Glass Fibers (GF), Aluminum Tread Plate (AP).

3. MECHANICAL AND X-RAY TESTS

3.1 Bending test

The bending test determines the flexural modulus, strength and fracture resistance of a material. It is a measure of the ability of a material to resist deformation under an applied load, in effect approximating conditions such as bending and sagging in structural applications. This is a critical test for materials intended to be used in a protective application where resistivity against bending forces is the metric.

The test samples were prepared according to ASTM D790 standards for flexural testing [30] with dimensions of 20 mm × 25 mm and 150 mm. To ensure reliability, five samples were tested, and the average results were reported.

A three-point bending test was conducted, where the specimen was supported at two ends, and a load was applied at the center until failure. The stress-strain curves were generated by recording load-displacement data, enabling the calculation of the flexural modulus and fracture strength.

3.2 Impact strength test

The impact strength test evaluates a material's ability to absorb energy during a high-speed impact. This property is critical for ballistic applications, where materials must withstand sudden forces and dissipate energy effectively.

Standards and Sample Dimensions:

(1) Layered Composite Samples: 100 mm × 20 mm × 25 mm, fabricated according to mold specifications.
(2) Adhesive Base Material Samples: 80 mm × 10 mm × 4 mm, following ASTM D6110-18 [31].

Five samples of each type were tested to ensure consistent results.

The test was conducted using a Charpy impact testing machine (Testing Machines Inc.). The samples were positioned in a predefined slot, and a pendulum hammer with a capacity of 50 J (for layered composites) and 7.5 J (for adhesive base materials) was released from a fixed height. The absorbed energy was calculated as the energy absorbed during the impact divided by the cross-sectional area of the sample.

3.3 Compressive strength test

The compressive strength test determines a material's ability to withstand compressive forces, essential for materials used in structural and protective applications. It measures the maximum stress a material can sustain before failure.

The samples were prepared with dimensions of 20 mm × 20 mm × 20 mm, according to ASTM D695 standards for compressive strength testing [32]. Five samples were tested, and the results were averaged for accuracy.

Testing was performed at room temperature (27°C) using a 100kN compression testing machine (manufactured by Laryee, China). Each sample was subjected to uniform loading, and stress-strain curves were recorded to analyze the material's compressive performance.

3.4 Hardness resistance test

The hardness test is the method of determining the resistance of a material to surface deformation or indentation. Surface durability is a key parameter for evaluating and is especially important in materials destined for high-impact or abrasive environments.

Standards and Sample Dimensions:

(1) Layered Composite Samples: Prepared according to the mold specification to 100 mm × 20 mm × 25 mm.
(2) Adhesive Base Material Samples: Specimen size is 80 mm × 10 mm × 4 mm, prepared according to ASTM D2240 standards [33]. Each configuration was tested in five samples, and the average values were calculated.

A Shore D hardness test was accomplished by using a standardized hardness tester. The proper positioning of the sample in the device and a needle penetrating the surface to measure the resistance were performed. Both composite and adhesive material samples were recorded for hardness values.

All mechanical tests, including impact, hardness,

compressive, and bending tests, were conducted with a minimum of five repetitions (n = 5) for each model. The results are presented as mean ± standard deviation to ensure statistical reliability and reproducibility. Descriptive statistical analysis was conducted using Microsoft Excel 2021. This approach aligns with standard material testing protocols and allows for accurate comparison between the two composite models.

Table 3 provides a summary of the mechanical tests conducted in this study, which provided insights into the performance of the materials under various conditions. All tests were performed using five samples per configuration, and the average results were reported to ensure reliability.

Table 3. Purpose of each mechanical test conducted in the study

Test	Objective	Standard	Sample Dimensions	Repetition
Bending Test	Evaluate flexural modulus and fracture resistance.	ASTM D790	150 mm × 20 mm × 25 mm	5 samples
Impact Strength Test	Assess energy absorption and toughness of materials.	ISO-180	100 mm × 20 mm × 25mm; 80 mm × 10 mm × 4 mm	5 samples
Compressive Strength	Determine material strength under compressive loads.	ASTM D695	20 mm × 20 mm × 20 mm	5 samples
Hardness Resistance	Evaluate surface hardness and resistance to indentation.	ISO-180	100 mm × 20 mm × 25 mm; 80 mm × 10 mm × 4 mm	5 samples

3.5 X-ray imaging test

X-ray imaging test is a non-destructive physical testing kind of method that can be applied to view the internal structure of a material. By applying the principles of X-ray physics, this method generates images that reveal density variations within the sample. This is critical for evaluating ballistic performance by determining whether a bullet has penetrated, remained embedded, or been completely stopped by the material.

When X-rays pass through a sample, they are absorbed at varying degrees depending on the density of the material. This differential absorption creates a detailed image of the internal layers on a detector screen.

The samples tested measured 20 × 20 cm² and included varying layer configurations as described in the mechanical tests section. Each sample was placed in the designated position within the X-ray testing device. Upon activation, the X-ray device emitted a beam of X-rays, which traveled through the sample and reached the detector on the opposite side. The resulting image displayed the internal structure of the composite, showing:

- Depth of bullet penetration.
- Whether the bullet was retained or exited the sample.
- Any internal damage, such as delamination or microfractures.

The X-ray imaging test was conducted using an X-ray machine manufactured by JPI Korea, specifically designed for material testing and ballistic evaluation. Appropriate radiation safety measures were implemented, including lead shielding and trained personnel, to ensure compliance with safety standards.

The X-ray images were analyzed visually. Measurements such as penetration depth (in mm) and damage radius (in mm) were recorded for each sample.

4. RESULTS AND DISCUSSION

4.1 Result of the bending test

The stress-strain curves for the five tested samples, as shown in Figure 2, highlight significant differences in their flexural performance. Sample 4 exhibited the highest peak stress, indicating its superior load-bearing capacity under bending. Its gradual failure beyond the peak stress suggests ductility and the ability to absorb significant energy before complete fracture. The initial slope of Sample 3 was steep, indicating high stiffness, and the broad plateau suggests its enhanced energy absorption capability and resistance to brittle failure. On the other hand, Samples 1 and 2 experienced earlier failure, with lower peak stresses, which signifies meager reinforcement and prompt crack spread. Sample 5, where the layer arrangement was reversed, had intermediate behavior, with moderate peak stress and a short plateau phase. The findings of these results highlight the impact of layer configuration and reinforcement type on the flexural behavior of composite materials.

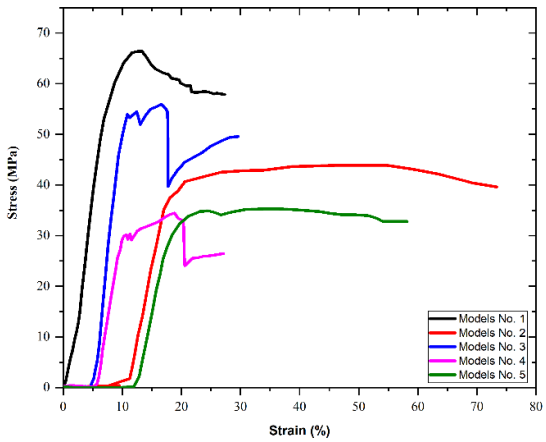

Figure 2. The stress-strain curves for the five tested samples highlight significant differences in their flexural performance

(a) Before the test

(b) After the test

Figure 3. Bending test samples

Figure 3 (a) shows the bending test samples prior to performing the test, following the pristine states of the samples, which are intact, uniform, and with well-defined layers. 1-5 are labeled samples, and the adhesive base material is on far left. On the other hand, Figure 3 (b) shows the same samples following the three-point bending test. The applied bending forces cause significant deformation, delamination, and fracture of the reinforcement layers as observed by the images. The samples exhibit considerable differences in the extent to which the damage is distributed over the laminates and these differences reflect differences in the flexural properties and structural integrity under stress. These results confirm the significance of reinforcement layer configuration on the performance of the bending.

A comparison of the flexural modulus of the samples, which is illustrated in Figure 4, provides additional support for the analysis of the stress-strain curves. Sample 4, with the highest modulus (~0.75 GPa), was achieved owing to the increased number of reinforcement layers and the combined stiffness of Kevlar and carbon fiber. Sample 3 followed closely with slightly lower modulus values as a result of fewer reinforcement layers, but its uniform stress distribution allowed it to exhibit superior energy dissipation. Sample 1 shows a lower modulus because of its low reinforcement, which reduced its ability to resist deformation. Despite its intermediate modulus, Sample 5 was successfully effective with stiffening due to its unique stacking configuration, but not as good as Sample 4.

The flexural strength results, as shown in Figure 4, also support the significance of the inclusion of reinforcement layers, and their configuration. Sample 3 had the best flexural strength (~66 MPa), as a result of a balanced configuration of the layers, where the load transfer was optimized and stress concentrations minimized. However, for Sample 4, which has the highest modulus, slightly lower flexural strength was observed compared to Sample 3, but this is likely caused by minor delamination at the layer interfaces. Although it had a slightly lower flexural strength, Sample 5 demonstrated the tradeoff incurred for the alternative stacking sequence and increased material stiffness. Samples 1 and 2 had significantly lower flexural strengths compared to those, which shows the reinforcement extent for sustaining the higher loads was insufficient.

The results proved that the mechanical performance of the composite materials depends on the amount, type, and pattern of the reinforcement layer. A synergy between Kevlar's toughness, carbon fiber's stiffness, and glass fiber's resistance to crack propagation proved critical to enhanced flexural properties. The addition of an aluminum front plate in all samples serves to distribute load and impact resistance, and adhesive matrix (79% UPS+1% PMMA+20% NR) is utilized to bond layers effectively. According to existing research on fiber-reinforced composites, the findings agree with those on fiber-matrix interactions and layer stacking, which greatly enhance the flexural properties.

The observed trends in flexural properties are further validated by comparison with previous studies. Kanitkar et al. [34] presented research on Kevlar reinforced composites with flexure strengths between 60-70 MPa, also closely matching the flexure strengths achieved by Samples 3 and 4 in this study [34]. For instance, Dong and Davies [35] also showed that the flexural moduli of carbon and glass fiber hybrid composites fell in the range of 0.7-0.9 GPa, conforming with the results of Sample 4. The improved performance exhibited by the samples with aluminum tread plates was explained through studies on aluminum reinforced composites, Haro et al. [21], where metallic layers play a role in increasing both the flexural stiffness and energy dissipation. However, unlike previous studies, this work uniquely combines multiple reinforcement layers with a polymer adhesive matrix, offering improved ductility and damage resistance, as evidenced by the stress-strain curves and X-ray imaging.

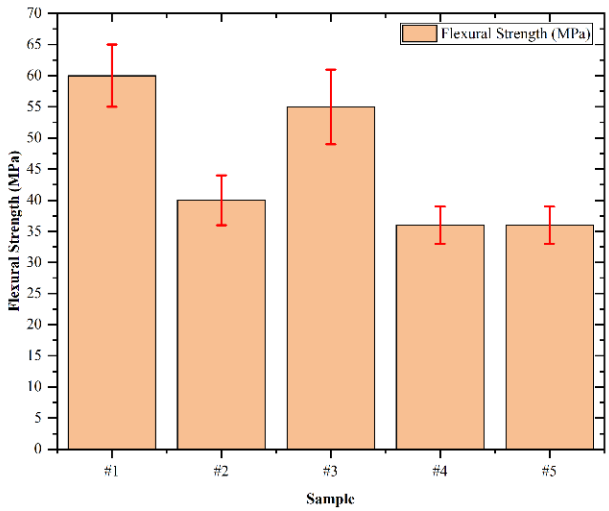

(a)

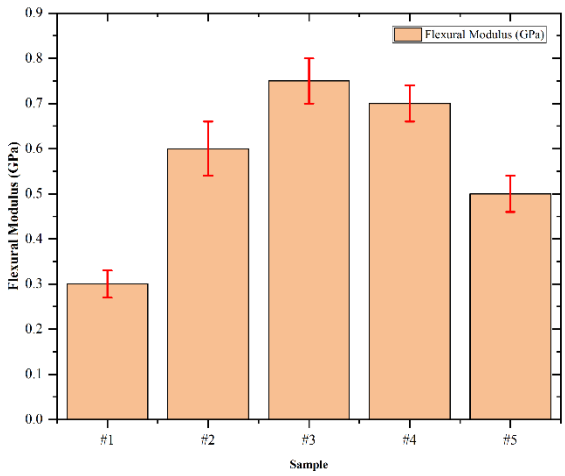

(b)

Figure 4. (a) Flexural strength comparison across the tested composite samples, illustrating the influence of different reinforcement configurations; (b) Comparative analysis of flexural modulus, showing variations in stiffness among the samples

4.2 Compression test results

The stress-strain curves for the five samples, as presented in Figure 5, reveal significant differences in their compressive performance. Sample 2 exhibited the highest peak compressive strength (~262.8 MPa), followed closely by Sample 3 (~217.8 MPa) and Sample 1 (~215.9 MPa). These samples demonstrated steeper slopes in the elastic region, indicative of higher stiffness and enhanced resistance to deformation. Conversely, Sample 4 displayed a lower peak strength (~117.9 MPa) but exhibited ductile behavior, characterized by a gradual failure over an extended strain range. Sample 5, with the lowest peak strength (~103.6 MPa), showed a less steep slope, highlighting reduced stiffness and limited resistance to compressive forces. The variations in mechanical performance can be attributed to differences in layer configurations, material composition, and interfacial bonding between reinforcement layers.

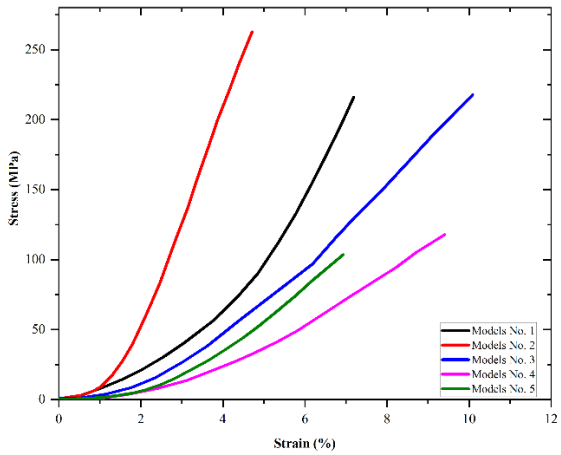

Figure 5. The stress-strain curves for the five tested samples highlight significant differences in their compression performance

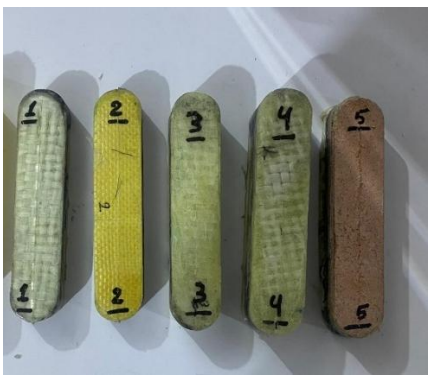

(a) Before test

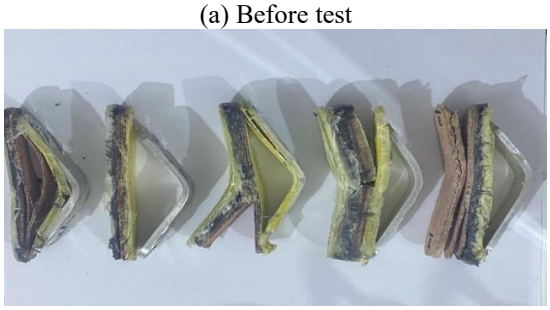

(b) After test

Figure 6. Impact test samples

Figure 6 (a) shows the impact test samples prior to testing with pristine condition with clear, intact reinforcement layers. All samples (labelled from 1 to 5) have a smooth surface and uniform thickness. After the impact test, Figure 6 (b) shows the same individual samples with substantial deformation, delamination, and fracture in the reinforcement layers. Damage patterns across the samples vary from signs of severe splitting and fiber breakage to just surface cracks. These results point to the variety of composite configurations that affect the impact resistance, and they demonstrate their dependence on reinforcement material and layering on energy absorption and structural integrity in impacts.

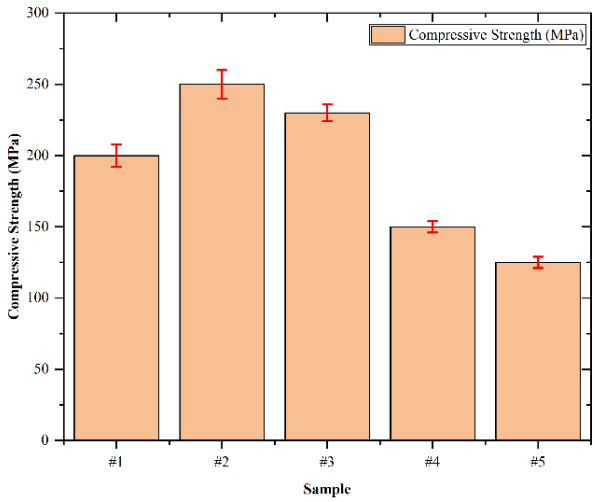

(a) Comparison of compressive strength (MPa)

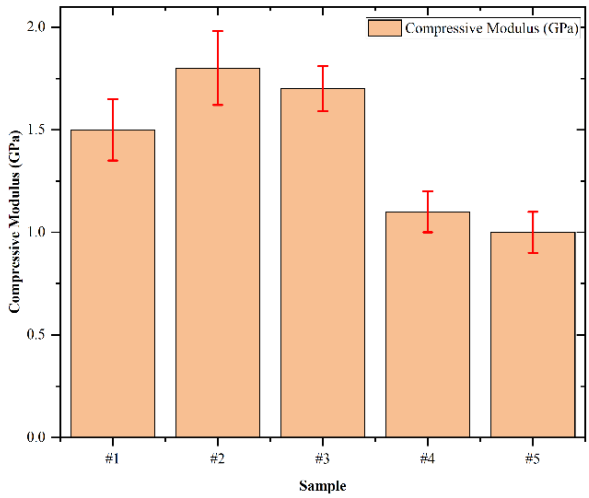

(b) Comparison of compressive modulus (GPa)

Figure 7. (a) Comparison of compressive strength across samples with error bars, showing variations in strength values for different samples; (b) Comparison of compressive modulus across samples with error bars, emphasizing differences in stiffness properties under compressive loads

The compressive strengths of the samples, as illustrated in Figure 7, emphasize the role of reinforcement density and stacking sequence in determining load-bearing capacity. Sample 2, with its optimized reinforcement configuration of Kevlar, carbon fibers, glass fibers, and natural leather, achieved superior compressive performance due to effective stress transfer and minimized interfacial delamination. While Sample 2 excels in compressive strength under static loads, its rigidity limits energy absorption under dynamic impacts,

leading to inferior impact performance compared to Sample 4, which is optimized for dynamic load scenarios. Sample 1 and Sample 3 had competitive strengths as Kevlar fibers and carbon fibers contributed to stiffness and energy absorption properties. Conversely, Sample 4 and Sample 5 exhibited lower performance, possibly stemming from a weaker interface bonding and/or suboptimal stacking sequences leading to localized stress concentrations and ahead of failure.

Further validation of the trends observed in the stress-strain curves is provided by the compressive modulus values presented in Figure 7. Sample 3 and Sample 2 exhibited higher modulus (~1.7 GPa and ~1.8 GPa) than Sample 1 (~1.523.00000000000000 GPa), implying superior stiffness. Lower modulus values of Sample 4 (~1.2 GPa) and Sample 5 (~1.0 GPa) further confirm the reduction in compressive strength based on reinforcement configuration. An optimized combination of reinforcement and an adhesive matrix is shown to increase both strength and stiffness.

The results obtained are in line with the results obtained in previous studies. A combination of compressive strengths of 250-270 MPa [36] suggests that this performance should be achieved in the Kevlar-carbon hybrid composites, as the performance of Sample 2 is comparably close. Similarly, Gupta et al. [37] pointed out that the glass fiber reinforcement increases the ductility under compressive load, consistent with the behavior encountered with Sample 4. In addition, as highlighted by Peterson et al. [38], the adhesive matrices are critical for the effective stress transfer, in agreement with the main conclusions of this study for the synthesis of the UPS-PMMA-NR adhesive blend.

The results in summary highlight the important yet frequently overlooked impact of the reinforcement layer build-up and material properties on the compressive performance. The best performing composite was Sample 2, which exhibited both high strength and high stiffness, and Sample 4, which performed favorably in regard to its excellent ductility, being ideal for applications that require energy dissipation. This work sheds light on how fiber composites used in high-performance applications can be designed.

4.3 Hardness test results

The hardness results yield useful insights into the effect both base material composition and reinforcement configuration have on the mechanical performance of the composites. A non-linear trend for the hardness (Shore D) variation with the PMMA volume fraction in a UPS-based matrix is shown in Figure 8. Maximum hardness of 58.2 Shore D occurs at 10% PMMA (decreasing with increasing concentrations from 10%), suggesting optimal reinforcement occurs at moderately low concentrations of PMMA. At lower concentrations (5%), the matrix lacks sufficient rigidity (~21.4 Shore D), while higher PMMA content (> 15%) likely introduces stress concentrators or compromises interfacial bonding, resulting in reduced hardness values.

Similarly, the addition of NR to the UPS-based matrix, as shown in Figure 8, demonstrates an increasing trend in hardness, with a maximum value (~86.3 Shore D) observed at 8% NR. Beyond this concentration, a slight decline in hardness suggests that excessive NR may reduce matrix stiffness. These findings highlight the role of NR in enhancing energy dissipation and reducing brittleness at intermediate concentrations, whereas overloading may weaken the overall structural integrity.

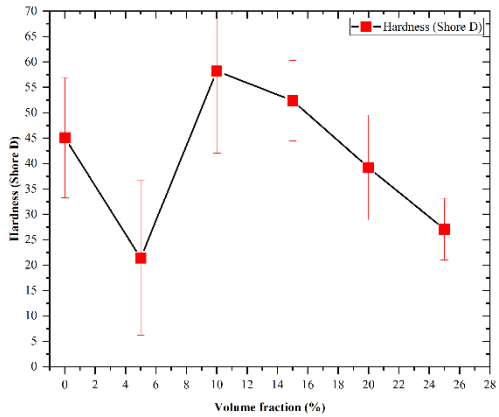

(a) Hardness as a function of PMMA

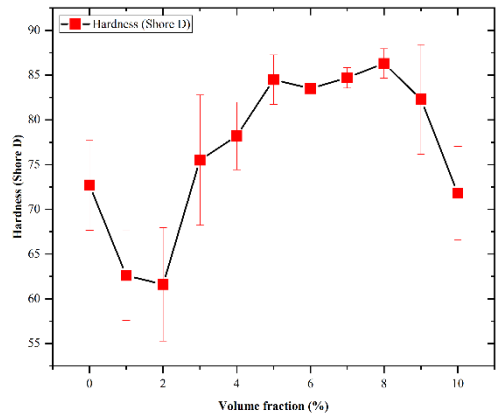

(b) Hardness as a function of NR

Figure 8. (a) Hardness as a function of Polymethyl methacrylate (PMMA) volume fraction, illustrating the variation in Shore D hardness with increasing PMMA content; (b) Hardness as a function of natural rubber (NR) volume fraction, highlighting changes in Shore D hardness with varying NR content

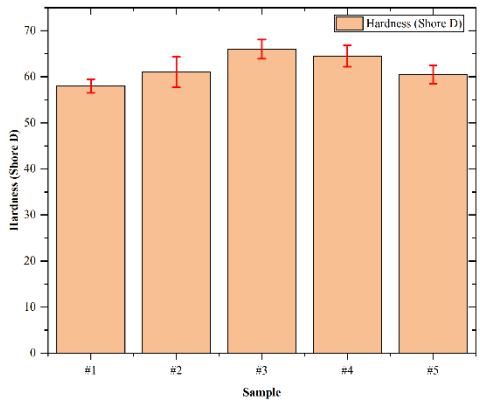

Figure 9. Hardness of samples with adjusted base material, including error bars to show variability in Shore D hardness measurements across the samples

The comparison of the composite samples using the optimized base material (79% UPS + 1% PMMA + 20% NR), as depicted in Figure 9, further emphasizes the importance of reinforcement configuration. Sample 3 exhibited the highest hardness (~66 Shore D), attributed to its optimized stacking sequence, which includes five layers of Kevlar fibers, carbon fibers, glass fibers, and tanned cowhide leather. This likely improved the load distribution as well as interfacial bonding

and resulted in a higher surface stiffness. Medium hardness values around or below 60-64.5 Shore D are seen in Samples 1, 2, and 4, a result of their slightly less effective reinforcement stacking. Differently, Sample 5 showed the lowest hardness (~58 Shore D), which is caused either by an inefficient stacking sequence or by a weak interfacial adhesion between the reinforcement layers.

These results are consistent with results from earlier studies. However, Negi et al. [39] describe that to obtain the best mechanical properties of polymer composites, reinforcement concentrations within the range of 5-10% are the most optimal, which is in accord with the trends found for PMMA and NR in this study. In addition, the functions of Kevlar and carbon fibers in improving the surface stiffness and impact resistance match well with the results demonstrated by Ganesamoorthy et al. [40], who stated the superior mechanical performance of the hybrid composites with the balanced distribution of reinforcement.

The results of this hardness test indicate that there exists an interdependence between the material constitution of the base material and the reinforcement configuration as to how the composite performance will be. In this sense, the base material is optimized, which, together with a well-thought-out stacking sequence, produces compressive mechanical properties suitable for applications where high surface stiffness and high impact resistance are required.

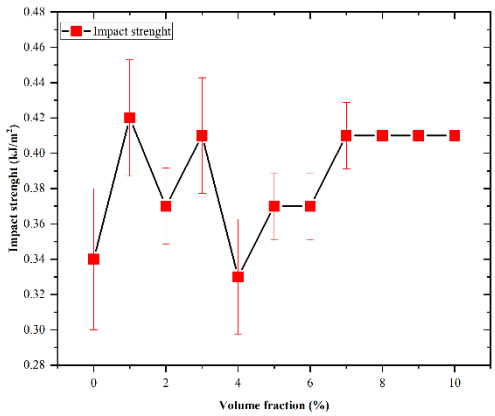

(a) Impact strength as a function of PMMA

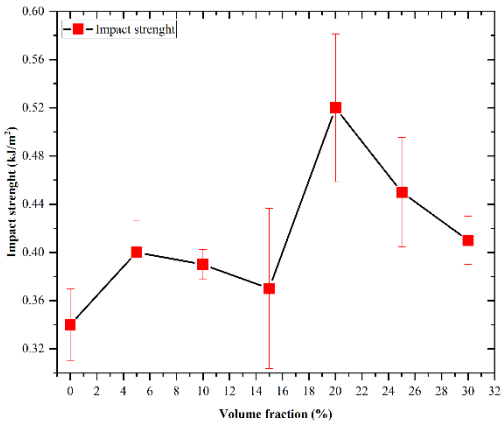

(b) Impact strength as a function of NR

Figure 10. (a) Impact strength as a function of Polymethyl methacrylate (PMMA) volume fraction, showing variations in impact strength with increasing PMMA content; (b) Impact strength as a function of natural rubber (NR) volume fraction, illustrating changes in impact resistance with varying NR content

4.4 Impact test results

The impact strength of the tested materials was analyzed in the three configurations, providing important information on the influence of base material composition and reinforcement layers. For a series of UPS as base material with varying PMMA volume fractions, the impact strength exhibited only moderate deviations and reached its highest value of 0.42 kJ/m² at 1% PMMA and remained practically constant in the range from 7% to 10%, as shown in Figure 10. This behavior indicates that very small amounts of PMMA actually increase matrix rigidity, resulting in enhanced impact resistance. Nevertheless, increasing PMMA fractions did not result in return on investment, nor did it enhance system performance any further, probable reasons being the brittleness of PMMA, thereby limiting energy absorption during impact events.

On the other hand, as revealed in Figure 10, varying NR volume fractions combined with UPS had a pronounced effect on impact strength, peaking at 0.52 kJ/m² at 20vol% NR. This is a result of NR's elastomeric properties, which allow good impact energy dissipation. The impact strength was found to decrease at loadings beyond 20%, which was thought to be a saturation effect of NR disrupting matrix uniformity and reducing mechanical integrity. These results demonstrate that NR is more effective in producing energy absorption than PMMA.

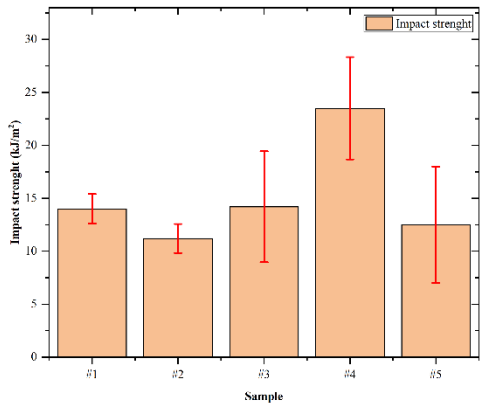

Figure 11. Impact strength of different supporting materials with adjusted properties, including error bars to represent the variability in impact resistance measurements for each sample

In the third configuration (using base material that is 79% UPS, 1% PMMA, 20% NR with reinforcement layers, Samples 1 through 5), much scatter in impact strength is observed, as evidenced in Figure 11. Sample 4 was the sample with the highest impact strength, followed by Samples 1 and 3, showing the positive effect of reinforcing layers towards the impact resistance. Sample 4 has superior performance due to its optimum arrangement and combination of Kevlar fiber, carbon fiber, and aluminum plates that absorb and redistribute impact energy effectively. Meanwhile, Sample 2 and Sample 5 exhibited comparatively lower impact strength, indicating that their reinforcement configurations were less effective in managing impact energy. The variability in impact strength across Samples 1–5 demonstrates the importance of reinforcement layer arrangements in determining energy absorption and redistribution. Strategic configurations, such as in Sample 4, ensure higher impact resistance. The trend depicted here demonstrates that layer arrangement and

material properties play a critical role in determining the impact performance of composite samples.

The results overall confirm the significance of base material composition and reinforcement layers to impact resistance optimization. These results suggest NR will absorb energy better than PMMA, owing to its elastic properties. Moreover, Sample 4 demonstrates how iterative and strategically layered reinforcement systems can accommodate robust combinations of energy absorption and structural integrity for impact resistance. Sample 4 mitigates failure mechanisms like spalling through its aluminum plate and prevents delamination with strong interfacial bonding, ensuring structural integrity under impact. The interplay between the reinforcement materials and the adhesive matrix proves critical in determining mechanical performance under both bending and impact forces. Optimizing both bending and impact properties requires a balanced layering of reinforcement materials, ensuring flexibility and stiffness while maintaining strong interfacial bonding for uniform load distribution. They are consistent with recent studies of hybrid reinforcement systems, and also suggest that tailored material designs can result in superior ballistic and impact resistance performance.

Comparison of mechanical tests across all samples has shown Sample 4 to have inherently very good performance, especially in terms of impact strength, a critical ballistic resistance parameter. The material's capacity to absorb and spread the kinetic energy from a high-velocity projectile, such as a 9 mm pistol bullet, is directly related to impact strength. Sample 4 (23.5 kJ/m²) showed superior impact strength due to its ability to spread impact energy among various composite layers and avoid local stress concentration, which significantly reduces potential failure of the material. It owes its high energy absorption capacity to the strategic combination of Kevlar fibers, carbon fibers, glass fibers, and aluminum plates arranged within its structure. The impact resistance of the crumple zone comes from high tensile strength Kevlar fibers, which can absorb energy by elongating the fibers, and an aluminum plate, which primarily acts to divert the energy of the bullet to a larger extent.

However, Sample 2, which has the highest compressive strength (262.77 MPa), shows low impact performance because it is incapable of absorbing and dissipating the most dynamic energy. Resistance to static forces is not as representative as the dynamic and high-velocity nature of ballistic impacts. Sample 2 is expected to perform well under gradual load conditions, due to its compressive strength; however, its low impact strength (11.2 kJ/m²) limits the ability to effectively manage sudden, high-energy impact loads. The anisotropy is likely due to the absence of a suitable arrangement of reinforcement layers that synergize as an energy absorber.

Sample 1 shows well-balanced structural integrity and energy absorption with its bending (66.09 MPa) and impact strength (14 kJ/m²). The reason for its performance is the interplay of its layers of reinforcement, especially Kevlar and carbon fibers. Although it is not as good as Sample 4 overall, its impact strength is marginally smaller, and it has a lesser interaction between its layers. Sample 1 could conceivably be a viable candidate for bending and impact property applications, yet would not offer the same degree of repeated or extreme ballistic impact protection as Sample 4.

Sample 4 is further superior in the sense that its structural configuration makes good use of the mechanical properties of its reinforcement materials. The Kevlar fiber is good at dissipating energy, serving as a first line of defense, carbon fibers provide overall strength and stiffness, and glass fibers and aluminum plate add additional stiffness and a barrier to penetration. Particularly, the aluminum plate contributes, by distributing kinetic energy across a larger surface area, to decreasing the depth of bullet penetration. Sample 4 is a result of this synergy of materials that is resisting the impact and further damage, such as spalling or delamination, common failure mechanisms in ballistic materials.

Finally, Sample 4 is concluded as the optimum choice for ballistic shields regarding 9mm pistol round resistance. It is also shown that its superior impact strength, as well as its balanced mechanical properties in other tests, make it an excellent choice to provide good protection. Both the mechanical and architectural structures exhibit an effective combination of energy absorption, structural rigidity, and surface damage resistance, which provides great promise for practical application in ballistic protection. These results confirm the need for considering both material selection and structural design for maximum performance of composite materials in high-performance applications.

4.5 Ballistic testing procedure and results

The ballistic performance of the fabricated body armor samples was evaluated in accordance with the NIJ-0101.06 standards, with detailed specifications of thickness and mass provided in Table 2. Testing was conducted using a Glock 17 pistol chambered for 9 × 19 mm full metal jacket (FMJ) rounds, aligned with the NIJ Level II threat category. Each bullet had a mass of 8.0 g and a round nose shape. The average muzzle velocity, measured using a Doppler radar-based velocity tracking system, was confirmed at 370 m/s. Tests were carried out at the Iraqi Police shooting range under controlled environmental conditions, including a relative humidity of 45 ± 5%. Firing distances began at 15 meters and were gradually reduced to a minimum of 2.6 meters to determine the closest range at which full penetration resistance could be maintained. All procedures were conducted under the supervision of trained field personnel to ensure standardized and safe testing protocol.

Post-ballistic testing, the samples underwent X-ray imaging to evaluate the internal structural damage, depth of penetration, and effectiveness of energy dissipation across the layers of the composite armor.

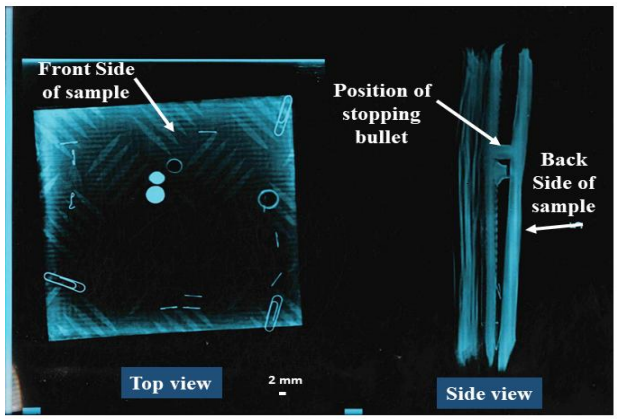

Figure 12. The X-ray imaging of the composite sample
Note: The top view highlights bullet impact points and the side view illustrates internal structural deformation and the bullet stopping position, confirming the material's effectiveness against a 9 mm bullet

The investigation of the ballistic performance of the bullet-resistant composite sample employs an important technique called X-ray imaging analysis that gives valuable information on the performance of the composite under ballistic impact. As visualized in Figure 12 of Sample 4, the marked difference from the top view is that the initial dispersion of energy impact is well evidenced by the holes on the frontal aluminium checker plate. The deformation patterns that surround the affected impact areas show that the composite absorbs and dissipates energy efficiently. This lack of complete perforation supports the conclusion that the sample can stop 9mm bullets in their tracks. The side view clearly shows internal structure distortion, while the outer shell adequately absorbed the shock, and the layers of Kevlar fibers, carbon fibers, and other materials did provide sufficient reinforcement and compressed and rerouted the energies imparted on impact. Most importantly, the layered configuration remained fairly cohesively intact while preserving its integrity from high-velocity stress objections that were not observed to separate delamination or tear of the adhesion matrix, compounded by the reinforcement layers. This imaging augments the mechanical testing outcomes, most notably the impact strength as observed during the test, to support its use in ballistic projects. The conclusions show that further research composes an ability to ensure a safe and stable defense against 9mm bullets. The imaging results confirm that Sample 4 exhibited the most effective resistance, with minimal depth of penetration and no complete breakthrough even at closer distances. These observations align with the superior impact strength and energy absorption capabilities demonstrated by Sample 4 in prior mechanical tests.

In comparing our findings on polymer-based composites for ballistic protection against existing studies, it becomes evident that the integration of advanced materials and strategic layering plays a pivotal role in achieving enhanced ballistic resistance. Research on polymer composite bullets, such as those introduced by PolyCase and Ruger, demonstrated the effectiveness of polymer and copper mixtures in creating lightweight yet high-performing ammunition [41]. These bullets, particularly the ARX designs, redirect hydraulic forces laterally to enhance terminal performance. While our study focuses on polymer-based armor rather than bullets, the insights into material behavior under ballistic stress emphasize the potential of polymer composites in high-impact applications. Similarly, studies on composite metal foams (CMFs) [42] revealed that CMFs, despite being lightweight, can disintegrate armor-piercing bullets with a thinner plate compared to conventional solid metals, demonstrating a superior weight-to-performance ratio. This finding aligns with our goal of developing lightweight yet robust composites for body armor [43].

The findings of this study represent a significant advancement in the design of hybrid composite materials for ballistic protection when compared to existing Kevlar-aluminum systems. Unlike prior research that primarily combined Kevlar with aluminum alloy and epoxy matrices-often enhanced with STFs or nano-fillers for improved energy dissipation [21, 44], our approach integrates a broader reinforcement strategy. Specifically, Sample 4 combines Kevlar, carbon, and glass fibers with cowhide leather and an aluminum checker plate, all bonded within a tailored UPS-PMMA-NR matrix. This unique configuration achieved high impact strength (23.5 kJ/m²) and effective bullet resistance per NIJ 0101.06 standards, without relying on STF or high-density foam. In contrast, aluminum foam systems with nano-reinforcements have shown improved ballistic performance but often at the cost of increased weight and reduced flexibility [45]. Furthermore, while other studies emphasize stacking sequences and fiber architecture as critical to impact behavior [46], the current work extends this by demonstrating that reinforcement synergy, layer orientation, and matrix design collectively govern the composite's resistance to penetration and internal damage, as validated by X-ray imaging. These results not only affirm the efficacy of layered hybrid composites but also underscore the potential of integrating unconventional reinforcements and optimized polymer matrices for next-generation ballistic armor.

The ballistic limit theory, which quantifies the minimum velocity required for projectile penetration, provides a valuable framework for contextualizing our results. Equations derived for laminates and homogeneous armor suggest that material composition and structural design critically influence ballistic performance. The predictive models, examining our empirical data, especially with regard to the superior impact resistance witnessed in Sample 4, can be further utilized to optimize the performance against various projectile calibers and velocities. The ballistic limit theory supports Sample 4's performance, as its hybrid reinforcement design maximizes energy dissipation, preventing localized stress accumulation and enhancing resistance. The highest impact strength (Sample 4) was obtained from a hybrid material configuration utilizing Kevlar fibers, carbon fibers, glass fibers, and an aluminum plate. Additionally, the composite, lightweight in nature, also exhibits excellent mechanical resistance, being suitable for personal protection in which mobility and robustness are indispensable.

Finally, we note that our results validate the findings of existing work emphasizing the role of material selection, structural design, and advanced layering techniques in ballistic protection. Sample 4 with the optimized hybrid reinforcement configuration provided proof of concept for polymer-based composites as an adequate solution for 9mm pistol bullet resistance. This work fills a critical gap by showing the effectiveness of adding multiple reinforcement layers to a polymer matrix-a route for future development of lightweight, high-performance ballistic armor.

5. CONCLUSION

This study successfully developed and characterized hybrid fiber-reinforced polymer composites for ballistic protection against 9 mm pistol rounds. A matrix composed of 79% UPS, 1% PMMA, and 20% natural rubber (NR) was combined with reinforcing layers including Kevlar fibers (KF), carbon fibers (CF), glass fibers (GF), tanned cowhide leather (CL), and aluminum plates (AP). Five distinct configurations were fabricated, and their mechanical and ballistic performance was systematically evaluated.

Among these, Sample 4 demonstrated superior overall performance. It achieved the highest impact strength of 23.5 kJ/m², a bending strength of 115.67 MPa, and compressive strength of 117.9 MPa, representing respective improvements of 67%, 75%, and 6% over the least performing configuration (Sample 5). Its Shore D hardness reached 64.5, indicating good surface rigidity, and it maintained its structural integrity after ballistic testing. The optimized stacking sequence of Sample 4, starting with aluminum and Kevlar layers for initial

energy absorption, followed by carbon and glass fibers for stiffness, and cowhide leather at the back for damping, proved critical in managing stress distribution and resisting penetration.

Ballistic testing in accordance with NIJ-0101.06 standards confirmed Sample 4's effectiveness in preventing full penetration from 9 mm bullets. X-ray imaging revealed projectile entrapment and progressive delamination, confirming superior energy absorption and resistance to spalling or catastrophic failure. The composite's configuration achieved a balance between flexibility, stiffness, and toughness, vital for personal protection equipment.

In summary, Sample 4 is a promising candidate for ballistic applications such as military and police vests. It offers an optimal weight-to-performance ratio, with improved energy dissipation and reduced backface deformation.

Although the developed hybrid composites showed promising mechanical and ballistic performance, long-term durability under environmental stressors such as UV exposure, moisture, and cyclic temperature remains to be evaluated. These factors are known to affect fiber–matrix interfacial bonding and mechanical stability. Also, the scalability of the fabrication process using hand lay-up and mechanical pressing requires further optimization for industrial application. Additionally, the cost of high-performance fibers such as Kevlar and carbon fibers may affect the economic feasibility for large-scale deployment. Future work will focus on:

- Incorporating SEM-based microstructural analysis to better understand fiber–matrix interfacial bonding,
- Evaluating multi-hit durability and environmental aging resistance (UV, humidity),
- And integrating numerical simulations and finite element analysis (FEA) to predict ballistic performance, optimize stacking sequences, and reduce experimental cost through virtual prototyping.

DATA CONSISTENCY AND CONFLICT OF INTEREST STATEMENT

The evidence of the findings of the present research aligns with the findings reported in the manuscript. All laboratory and field experimental measurements were carried out under controlled conditions per the specified ASTM and NIJ standards. The datasets produced and considered in the present study can be obtained by the relevant author on a reasonable request basis. No data were omitted or chosen to report.

The authors confirm that they have no interest in the publication of this manuscript. No commercial or financial relations that could be deemed as a possible conflict of interest existed in the conduct of the research.

REFERENCES

[1] Das, S., Prathasana, K., Nitin, P.A., JayaPriya, K.R.L., Mathivanan, V. (2025). Protection from ballistic threats: An exploration of textile materials for bullet-resistant outerwear. Zastita Materijala, 66(1): 5-14. https://doi.org/10.62638/ZasMat1202

[2] Selim, M.S., El-Safty, S.A., Shenashen, M.A., Elmarakbi, A. (2024). Advances in polymer/inorganic nanocomposite fabrics for lightweight and high-strength armor and ballistic-proof materials. Chemical Engineering Journal, 493: 152422. https://doi.org/10.1016/j.cej.2024.152422

[3] Nurazzi, N.M., Asyraf, M.R.M., Khalina, A., Abdullah, N., Aisyah, H.A., Rafiqah, S.A., Sabaruddin, F.A., Kamarudin, S.H., Norrrahim, M.N.F., Ilyas, R.A, Sapuan, S.M. (2021). A review on natural fiber reinforced polymer composite for bullet proof and ballistic applications. Polymers, 13(4): 646. https://doi.org/10.3390/polym13040646

[4] Elgohary, D.H. (2024). Technological aspects of body armour textiles for ballistic protection application. The Journal of the Textile Institute, 1-15. https://doi.org/10.1080/00405000.2024.2343162

[5] Peng, L., Zhou, J., Wang, Q.Y., Zhang, X.F., Guan, Z.W. (2024). Numerical modelling of the ballistic impact response of hybrid composite structures. Composites Part C: Open Access, 14: 100474. https://doi.org/10.1016/j.jcomc.2024.100474

[6] Tsirogiannis, E.C., Daskalakis, E., Vogiatzis, C., Psarommatis, F., Bartolo, P. (2024). Advanced composite armor protection systems for military vehicles: Design methodology, ballistic testing, and comparison. Composites Science and Technology, 251: 110486. https://doi.org/10.1016/j.Compscitech.2024.110486

[7] Braga, F.D.O., Lima, É.P., Lima, E.D.S., Monteiro, S.N. (2017). The effect of thickness on aramid fabric laminates subjected to 7.62mm ammunition ballistic impact. Materials Research, 20: 676-680. https://doi.org/10.1590/1980-5373-MR-2016-0883

[8] Samir, N.S., Radwan, M.A., Sadek, M.A., Elazab, H.A. (2018). Preparation and characterization of bullet-proof vests based on polyamide fibers. International Journal of Engineering and Technology (UAE), 7(3): 1290-1294. https://doi.org/10.14419/ijet.v7i3.13175

[9] Saleem, I.A., Ahmed, P.S., Abed, M.S. (2022). Experimental and numerical investigation of Kevlar and UHMWPE multi-Layered armors against ballistic impact. Materials Today: Proceedings, 56: 2516-2524. https://doi.org/10.1016/j.matpr.2021.08.345

[10] Khalaf, W.A., Hamzah, M.N. (2024). Experimental and numerical studies of ballistic resistance of hybrid sandwich composite body armor. Open Engineering, 14(1): 20220543. https://doi.org/10.1515/eng-2022-0543

[11] Morghode, D.S., Thakur, D.G., Salunkhe, S., Cepova, L., Abouel Nasr, E. (2024). Numerical study on the optimized thickness of layer configuration against the 7.62 APM2 projectile. Frontiers in Mechanical Engineering, 10: 1322640. https://doi.org/10.3389/fmech.2024.1322640

[12] Luz, F.S.D., Garcia Filho, F.D.C., Oliveira, M.S., Nascimento, L.F.C., Monteiro, S.N. (2020). Composites with natural fibers and conventional materials applied in a hard armor: A comparison. Polymers, 12(9): 1920. https://doi.org/10.3390/polym12091920

[13] Alkhatib, F., Mahdi, E., Dean, A. (2021). Design and evaluation of hybrid composite plates for ballistic protection: Experimental and numerical investigations. Polymers, 13(9): 1450. https://doi.org/10.3390/polym13091450

[14] Awad, S.K., Bdaiwi, W. (2024). Enhancing mechanical performance of PMMA resin through cinnamon particle reinforcement. Revue des Composites et des Materiaux

Avances, 34(3): 379. https://doi.org/10.18280/rcma.340313
[15] Athawale, A.A., Pandit, J.A. (2019). Unsaturated polyester resins, blends, interpenetrating polymer networks, composites, and nanocomposites: State of the art and new challenges. Unsaturated Polyester Resins, 1-42. https://doi.org/10.1016/B978-0-12-816129-6.00001-6
[16] Bhuvaneswary, M.G., Thachil, E.T. (2008). Blends of natural rubber with unsaturated polyester resin. International Journal of Polymeric Materials, 57(6): 543-554. https://doi.org/10.1080/00914030701818272
[17] Dong, J.P., Huang, J.G., Lee, F.H., Roan, J.W., Huang, Y.J. (2004). Effects of poly (methyl methacrylate)-Based low-Profile additives on the properties of cured unsaturated polyester resins. I. Miscibility, curing behavior, and glass-Transition temperatures. Journal of Applied Polymer Science, 91(5): 3369-3387. https://doi.org/10.1002/app.13557
[18] Costa, U.O., Nascimento, L.F.C., Garcia, J.M., Monteiro, S.N., Luz, F.S.D., Pinheiro, W.A., Garcia Filho, F.D.C. (2019). Effect of graphene oxide coating on natural fiber composite for multilayered ballistic armor. Polymers, 11(8): 1356. https://doi.org/10.3390/polym11081356
[19] Rosa, V.M., Felisberti, M.I. (2001). Unsaturated polyester resin modified with poly (organosiloxanes). I. Preparation, dynamic mechanical properties, and impact resistance. Journal of Applied Polymer Science, 81(13): 3272-3279. https://doi.org/10.1002/app.1783
[20] Fonseca, V.M., Oliveira, E., Lima, P.T., Carvalho, L.H. (2018). Development of Kevlar composites for ballistic applications. In 4th Brazilian Conference on Composite Materials, pp. 548-553. https://doi.org/10.21452/bccm4.2018.09.04
[21] Haro, E.E., Szpunar, J.A., Odeshi, A.G. (2016). Ballistic impact response of laminated hybrid materials made of 5086-H32 aluminum alloy, epoxy and Kevlar® fabrics impregnated with shear thickening fluid. Composites Part A: Applied Science and Manufacturing, 87: 54-65. https://doi.org/10.1016/j.compositesa.2016.04.007
[22] Purushothaman, A., Coimbatore, G., Ramkumar, S.S. (2013). Soft body armor for law enforcement applications. Journal of Engineered Fibers and Fabrics, 8(2): 155892501300800212. https://doi.org/10.1177/155892501300800212
[23] Nayak, S.Y., Sultan, M.T.H., Shenoy, S.B., Kini, C.R., Samant, R., Shah, A.U.M., Amuthakkannan, P. (2022). Potential of natural fibers in composites for ballistic applications–A review. Journal of Natural Fibers, 19(5): 1648-1658. https://doi.org/10.1080/15440478.2020.1787919
[24] Nascimento, L.F.C., Louro, L.H.L., Monteiro, S.N., Gomes, A.V., Marçal, R.L.S.B., Lima, É.P., Margem, J.I. (2017). Ballistic performance of mallow and jute natural fabrics reinforced epoxy composites in multilayered armor. Materials Research, 20: 399-403. https://doi.org/10.1590/1980-5373-MR-2016-0927
[25] Naveen, J., Jayakrishna, K., Hameed Sultan, M.T.B., Amir, S.M.M. (2020). Ballistic performance of natural fiber based soft and hard body armour-A mini review. Frontiers in Materials, 7: 608139. https://doi.org/10.3389/fmats.2020.608139
[26] Bichang'a, D.O., Aramide, F.O., Oladele, I.O., Alabi, O.O. (2022). A review on the parameters affecting the mechanical, physical, and thermal properties of natural/synthetic fibre hybrid reinforced polymer composites. Advances in Materials Science and Engineering, 2022(1): 7024099. https://doi.org/10.1155/2022/7024099
[27] Mohammed, R.F., Bdaiwi, W. (2025). Novel fiber-reinforced composites for lightweight ballistic protection: A structural and performance study. Revue des Composites et des Matériaux Avancés-Journal of Composite and Advanced Materials, 35(1): 51-62. https://doi.org/10.18280/rcma.350107
[28] Bandaru, A.K., Vetiyatil, L., Ahmad, S. (2015). The effect of hybridization on the ballistic impact behavior of hybrid composite armors. Composites Part B: Engineering, 76: 300-319. https://doi.org/10.1016/j.compositesb.2015.03.012
[29] Kacan, Y.O., Elaldi, F. (2020). Ballistic performance of unidirectionally oriented carbon fiber reinforced composite armor with high-Velocity impact. Journal of Reinforced Plastics and Composites, 39(19-20): 733-741. https://doi.org/10.1177/0731684420929084
[30] ASTM International. (2017). Standard test methods for flexural properties of unreinforced and reinforced plastics and electrical insulating materials. https://store.astm.org/d0790-17.html.
[31] ASTM International. (2018). Standard test method for determining the Charpy impact resistance of notched specimens of plastics. https://www.astm.org/d6110-18.html.
[32] ASTM International. (2023). Standard test method for compressive properties of rigid plastics. https://www.astm.org/d0695-15.html.
[33] ASTM International. (2021). Standard test method for rubber property-durometer hardness. https://www.astm.org/d2240-15r21.html.
[34] Kanitkar, Y.M., Kulkarni, A.P., Wangikar, K.S. (2016). Investigation of flexural properties of glass-Kevlar hybrid composite. European Journal of Engineering and Technology Research, 1(1): 25-29. https://doi.org/10.24018/ejeng.2016.1.1.90
[35] Dong, C., Davies, I.J. (2013). Flexural properties of glass and carbon fiber reinforced epoxy hybrid composites. Proceedings of The Institution of Mechanical Engineers, Part L: Journal of Materials: Design and Applications, 227(4): 308-317. https://doi.org/10.1177/1464420712459396
[36] Soupionis, G., Zoumpoulakis, L. (2021). Reinforced concrete structures containing chopped carbon fibers with polymer composite materials. Polymers, 13(21): 3812. https://doi.org/10.3390/polym13213812
[37] Gupta, S., Kumar, P., Srivastava, V.K. (2019). Stress field analysis of polymer composite with orthogonally reinforced fibers. Journal of Material Science and Technology Research, 6: 34-38. https://doi.org/10.31875/2410-4701.2019.06.5
[38] Peterson, A.M., Jensen, R.E., Palmese, G.R. (2011). Thermoreversible and remendable glass-Polymer interface for fiber-reinforced composites. Composites Science and Technology, 71(5): 586-592. https://doi.org/10.1016/j.compscitech.2010.11.022
[39] Negi, A.S., Katiyar, J.K., Kumar, S., Kumar, N., Patel, V.K. (2019). Physicomechanical and abrasive wear properties of hemp/Kevlar/carbon reinforced hybrid epoxy composites. Materials Research Express, 6(11):

115304. https://doi.org/10.1088/2053-1591/ab438d
[40] Ganesamoorthy, R., Meenakshi Reddy, R., Raja, T., Panda, P.K., Dhoria, S.H., Nasif, O., Jenish, I. (2021). Studies on mechanical properties of kevlar/napier grass fibers reinforced with polymer matrix hybrid composite. Advances in Materials Science and Engineering, 2021(1): 6907631. https://doi.org/10.1155/2021/6907631
[41] Marsh, G. (2017). Ballistic composites-protecting the protectors. Reinforced Plastics, 61(2): 96-99. https://doi.org/10.1016/j.repl.2015.10.003
[42] Garcia-Avila, M., Portanova, M., Rabiei, A. (2015). Ballistic performance of composite metal foams. Composite Structures, 125: 202-211. https://doi.org/10.1016/j.compstruct.2015.01.031
[43] Marx, J., Portanova, M., Rabiei, A. (2019). Ballistic performance of composite metal foam against large caliber threats. Composite Structures, 225: 111032. https://doi.org/10.1016/j.compstruct.2019.111032
[44] Syifa, S., Ariaty, M., Syahrial, A.Z., Pramono, A. (2024). The effect of alumina nanoparticles impregnated kevlar on ballistic resistance of aluminum alloy 7075 hybrid laminate composite for armor application. International Journal of Technology, 15(1). https://doi.org/10.14716/ijtech.v15i1.6050
[45] Haro, E.E., Odeshi, A.G., Castellanos, S., Sanchez, X., Abatta, L., Criollo, L., Alban, A., Szpunar, J.A. (2023). Ballistic impact performance of hybrid composite armors made of aluminum foam containing the dispersion of shear thickening fluid made of various synthetic nano-Fillers. Composites Part C: Open Access, 12: 100420. https://doi.org/10.1016/j.jcomc.2023.100420
[46] Bandaru, A.K., Ahmad, S., Bhatnagar, N. (2017). Ballistic performance of hybrid thermoplastic composite armors reinforced with Kevlar and basalt fabrics. Composites Part A: Applied Science and Manufacturing, 97: 151-165. https://doi.org/10.1016/j.compositesa.2016.12.007

NOMENCLATURE

UPS	Unsaturated polyester resin
PMMA	Polymethyl methacrylate
NR	Natural rubber
KF	Kevlar fibers
CF	Carbon fibers
CL	Cowhide leather
AP	Aluminum checker plate
PMEK	Methyl ethyl ketone peroxide
GPa	Gigapascal, a unit of stress
MPa	Megapascal, a unit of stress
ASTM	American Society for Testing and Materials standards